International Journal of Thermophysics, Vol. 25, No. 1, January 2004 (© 2004)

Viscosity of Gaseous Mixtures of HFC-134a (1,1,1,2-Tetrafluoroethane) + HFC-32 (Difluoromethane)

C. Yokoyama,[1,2] T. Nishino,[1] and M. Takahashi[1]

Received January 14, 2003

This paper reports experimental results for the viscosity of gaseous mixtures of HFC-134a (1,1,1,2-tetrafluoroethane) + HFC-32 (difluoromethane). The measurements were carried out with an oscillating-disk viscometer of the Maxwell type at temperatures from 298.15 to 423.15 K. The viscosity was measured for three mixtures containing 25.00, 52.40, and 74.98 mole% HFC-134a in HFC-32. Experimental results for the viscosity at normal pressures show a minimum as plotted against mole fraction in the higher temperature region, which may be the first experimental observation of the minima for dilute binary gaseous mixtures of HFCs. The viscosity at normal pressures was analyzed with the extended law of corresponding states developed by Kestin et al., and the scaling parameters were obtained for unlike-pair interactions between HFC-32 and HFC-134a. The modified Enskog theory developed by Vesovic and Wakeham was applied to predict the viscosity for the binary gaseous mixtures under pressure. As for the calculation of pseudo-radial distribution functions in mixtures, a method based on the equation of state for hard-sphere fluid mixtures proposed by Carnahan–Starling was applied.

KEY WORDS: binary mixture; corresponding states; Enskog theory; HFC-32; HFC-134a; mixture model; viscosity.

1. INTRODUCTION

Potential alternatives for the chlorofluorocarbons (CFCs) and hydrochlorofluorocarbons (HCFCs) are the hydrofluorocarbons (HFCs), such as HFC-125 (pentafluoroethane), HFC-134a (1,1,1,2-tetrafluoroethane), HFC-143a (1,1,1-trifluoroethane), and HFC-32 (difluoromethane), and their binary and/or ternary mixtures.

---

[1] Institute of Multidisciplinary Research for Advanced Materials (IMRAM), Tohoku University, Katahira 2-1-1, Sendai 980-8577, Japan.

[2] To whom correspondence should be addressed. E-mail: chiaki@tagen.tohoku.ac.jp

Transport properties, such as viscosity and thermal conductivity, of the alternative refrigerants influence the economic feasibility of heat exchangers that can perform close to the theoretical efficiency of thermodynamic cycles using CFCs. Therefore, reliable prediction methods for the transport properties of mixed HFCs are required to establish the process design methodology for a search of the optimum operating conditions of refrigeration systems using HFCs.

In our previous studies, we measured the gaseous viscosity of HFC-32, HFC-134a, HFC-143a, HFC-125 [1–4], HFC-125/134a [5], and HFC-125/32 [6] systems. As part of a continuing study of the viscosity of dense fluid systems containing HFCs, measurements of the viscosity of gaseous mixtures of HFC-134a + HFC-32, made at 298.15, 323.15, 348.15, 373.15, 398.15, and 423.15 K over a pressure range from 0.1 MPa to near the vapor pressure under subcritical temperature conditions or up to 7.6 MPa under supercritical temperature conditions, are reported in this paper. The viscosity data at 0.1 MPa were used to determine the scaling parameters of the unlike-pair interactions between HFC-32 and HFC-134a from the extended law of corresponding states [7]. The viscosity data under pressures were analyzed with the extended Enskog theory developed by Vesovic and Wakeham [8]. The pseudo-radial distribution function for species i and j in the mixture needed in the viscosity prediction was calculated from the numerical method based on the equation of state for hard-sphere fluid mixtures proposed by Carnahan and Starling [9].

2. EXPERIMENTAL

The viscosity was measured with an oscillating-disk viscometer of the Mawell type. The gas density at the experimental conditions of the viscosity measurement was measured with a high-pressure gas pipette. The experimental apparatus and procedures were the same as those described in previous studies [10–12]. The apparatus constant of the viscometer at the experimental temperature and pressure conditions was determined by considering the viscosity data of nitrogen taken from Stephan et al. [13] and the nitrogen gas density data from Jacobsen et al. [14]. As for the gas density determination, the second virial coefficient data for the HFC-134a/32 binary gas mixture reported by Weber [15, 16] were used to determine the gas compressibility factor values at the expanded conditions in a glass cylinder in the gas density measurement apparatus [10, 11]. While this method can give reliable density values, its reliability is uncertain for the case of ternary-component mixtures (e.g., R404A, R407C) that will be our next target. Therefore, we obtained the density values for the HFC-134a/32 binary gas mixtures from the equation of state model compiled in

Table I. Experimental Viscosity Values for the HFC-134a(1)+HFC-32(2) System

T (K)	P (MPa)	ρ ($kg \cdot m^{-3}$)	η ($\mu Pa \cdot s$)
	$x_{HFC\text{-}134a} = 0.2500$		
298.15	0.1007	2.659	12.10
	0.1971	5.278	12.07
	0.2929	7.959	12.04
	0.3941	10.88	12.00
	0.4913	13.78	12.01
	0.6020	17.21	11.97
	0.7073	20.61	11.96
	0.8045	23.88	11.95
	0.9034	27.36	11.94
	1.0054	31.11	11.93
	1.0974	34.67	11.92
323.15	0.1016	2.466	13.12
	0.2458	6.061	13.10
	0.3937	9.870	13.08
	0.5414	13.81	13.07
	0.6863	17.82	13.05
	0.8804	23.43	13.05
	1.0212	27.70	13.06
	1.1765	32.63	13.06
	1.3202	37.41	13.09
	1.4644	42.45	13.11
	1.6183	48.15	13.13
	1.7676	54.03	13.19
	1.9049	59.81	13.21
	2.0513	66.43	13.27
	2.1789	72.66	13.34
348.15	0.1011	2.272	14.16
	0.2950	6.736	14.15
	0.4924	11.43	14.12
	0.6866	16.22	14.14
	0.8826	21.23	14.15
	1.0786	26.43	14.14
	1.2679	31.66	14.17
	1.4607	37.21	14.22
	1.6648	43.37	14.25
	1.8641	49.68	14.33
	2.0614	56.26	14.37
	2.2287	62.14	14.43
	2.4553	70.59	14.52
	2.6482	78.31	14.66
	2.8103	85.22	14.74
	3.0056	94.17	14.90
	3.1674	102.2	15.03
	3.3196	110.4	15.18
348.15	3.4840	120.0	15.38
	3.6384	130.0	15.61
373.15	0.1015	2.124	15.16
	0.2992	6.341	15.17
	0.5498	11.85	15.15
	0.8412	18.48	15.20
	1.1431	25.66	15.23
	1.4434	33.12	15.29
	1.7775	41.85	15.34
	2.0276	48.72	15.42
	2.3338	57.55	15.51
	2.6209	66.30	15.63
	2.8889	74.95	15.78
	3.2424	87.15	15.97
	3.5429	98.35	16.18
	3.8525	110.8	16.43
	4.1936	126.0	16.77
	4.5033	141.2	17.16
	4.7943	157.1	17.59
	5.0144	170.3	17.96
	5.2740	188.1	18.53
	5.4829	204.0	19.04
	5.8053	232.8	20.10
	6.1593	273.1	21.74
	6.3196	295.7	22.72
398.15	0.1013	1.984	16.17
	0.2982	5.899	16.19
	0.4886	9.760	16.22
	0.6953	14.04	16.22
	1.0108	20.75	16.22
	1.3273	27.72	16.30
	1.6322	34.68	16.38
	1.9213	41.51	16.43
	2.2103	48.59	16.51
	2.5466	57.15	16.63
	2.8724	65.82	16.76
	3.2425	76.16	16.93
	3.5502	85.19	17.08
	3.9192	96.58	17.34
	4.2719	108.1	17.54
	4.5814	118.8	17.82
	4.9076	130.8	18.10
	5.2221	143.0	18.43
	5.5150	155.1	18.79
	5.8213	168.5	19.14

Table I. *(Continued)*

T (K)	P (MPa)	ρ (kg · m^{-3})	η (μPa · s)	T (K)	P (MPa)	ρ (kg · m^{-3})	η (μPa · s)
398.15	6.1306	183.0	19.61	323.15	0.7700	24.87	12.87
	6.4214	197.5	20.09		0.9778	32.65	12.88
	6.7501	215.2	20.52		1.1237	38.48	12.89
423.15	0.1016	1.871	17.19		1.2761	44.95	12.92
	0.3189	5.923	17.18		1.4175	51.36	12.94
	0.8803	16.73	17.25		1.5560	58.10	12.98
	1.2912	24.96	17.32		1.7164	66.61	13.06
	1.7218	33.91	17.37		1.8512	74.49	13.13
	2.1202	42.50	17.51	348.15	0.1018	2.777	13.93
	2.5254	51.56	17.59		0.1022	2.788	13.90
	2.8520	59.13	17.72		0.2359	6.517	13.93
	3.3579	71.33	17.91		0.3857	10.81	13.91
	3.6482	78.62	18.05		0.5833	16.68	13.93
	3.9513	86.46	18.21		0.7801	22.78	13.94
	4.2389	94.14	18.34		0.9709	28.96	13.95
	4.5636	103.1	18.53		1.1739	35.85	13.99
	4.8428	111.1	18.76		1.3652	42.69	14.04
	5.1453	120.0	18.95		1.5628	50.16	14.09
	5.3861	127.3	19.14		1.7705	58.50	14.16
	5.7115	137.5	19.41		1.9657	66.89	14.26
	6.0139	147.4	19.67		2.1922	77.42	14.39
	6.2785	156.3	19.93		2.4009	88.05	14.53
	6.6479	169.2	20.34		2.6038	98.47	14.71
	6.8715	177.3	20.60		2.7537	108.8	14.87
	7.1447	187.5	20.90		2.9198	120.2	15.10
	7.3575	195.7	21.22		3.1309	137.1	15.44
	7.5631	203.8	21.47	373.15	0.1006	2.555	14.91
					0.2932	7.552	14.93
	$x_{\text{HFC-134a}} = 0.5240$				0.4861	12.70	14.91
298.15	0.1034	3.319	11.84		0.6830	18.12	14.93
	0.1997	6.515	11.81		0.8736	23.54	14.96
	0.2958	9.817	11.80		1.0725	29.38	14.98
	0.3909	13.20	11.80		1.2780	35.63	15.03
	0.4885	16.82	11.78		1.5375	43.87	15.10
	0.5746	20.14	11.76		1.7652	51.46	15.18
	0.6921	24.89	11.74		1.9838	59.09	15.26
	0.7828	28.75	11.72		2.1779	66.18	15.35
	0.9180	34.89	11.73		2.3986	74.65	15.46
	0.9478	36.32	11.75		2.5858	82.20	15.58
323.15	0.1014	2.989	12.95		2.7402	88.72	15.70
	0.1016	2.995	12.93		2.9378	97.49	15.85
	0.2457	7.374	12.91		3.1940	109.7	16.07
	0.3874	11.85	12.88		3.3520	117.7	16.25
	0.5395	16.84	12.89		3.5674	129.4	16.50
	0.6817	21.73	12.87		3.7520	140.3	16.77

Table I. *(Continued)*

T (K)	P (MPa)	ρ (kg·m^{-3})	η (μPa·s)	T (K)	P (MPa)	ρ (kg·m^{-3})	η (μPa·s)
	3.9290	151.6	17.04	423.15	4.5932	131.2	18.85
	4.0904	162.7	17.33				
398.15	0.1020	2.424	15.86		$x_{HFC\text{-}134a} = 0.7498$		
	0.2918	7.011	15.87	298.15	0.1024	3.767	11.79
	0.4896	11.90	15.91		0.1933	7.236	11.78
	0.6454	15.83	15.95		0.2868	10.94	11.75
	0.8665	21.55	15.94		0.3715	14.43	11.73
	1.0761	27.11	15.98		0.4623	18.32	11.71
	1.2693	32.38	16.02		0.5741	23.36	11.69
	1.4588	37.68	16.07		0.6747	28.17	11.65
	1.6633	43.55	16.13		0.7627	32.63	11.63
	1.8646	49.51	16.19	323.15	0.1010	3.411	12.76
	2.0620	55.52	16.28		0.2032	6.962	12.75
	2.2945	62.83	16.33		0.2986	10.37	12.73
	2.4529	67.97	16.44		0.4298	15.23	12.73
	2.6395	74.20	16.55		0.5814	21.10	12.70
	2.8325	80.84	16.66		0.7295	27.15	12.70
	3.0859	89.92	16.83		0.8734	33.37	12.73
	3.2874	97.44	16.94		1.0200	40.10	12.74
	3.5057	105.9	17.13		1.1654	47.26	12.76
	3.7207	114.6	17.32		1.2967	54.21	12.79
	3.9260	123.3	17.52	348.15	0.1018	3.181	13.70
	4.1417	132.9	17.73		0.1032	3.225	13.71
	4.3295	141.6	17.96		0.2168	6.858	13.69
	4.5150	150.5	18.19		0.3516	11.29	13.70
	4.5956	154.6	18.28		0.4986	16.27	13.70
423.15	0.1014	2.265	16.80		0.6423	21.32	13.70
	0.3427	7.739	16.85		0.7886	26.64	13.72
	0.5765	13.16	16.85		0.9340	32.14	13.75
	0.8318	19.22	16.88		1.0848	38.09	13.77
	1.0765	25.17	16.95		1.2332	44.22	13.81
	1.3263	31.39	16.99		1.3857	50.82	13.87
	1.5658	37.51	17.06		1.5289	57.35	13.93
	1.8106	43.92	17.14		1.6809	64.68	13.99
	2.0458	50.24	17.21		1.8321	72.43	14.08
	2.2924	57.05	17.34		1.9792	80.51	14.20
	2.5334	63.88	17.43		2.1424	90.20	14.32
	2.7391	69.86	17.47		2.3190	101.8	14.49
	2.9687	76.71	17.66		2.4272	109.6	14.63
	3.2540	85.48	17.74		2.5461	118.9	14.80
	3.4831	92.76	17.90	373.15	0.1000	2.908	14.67
	3.7604	101.8	18.14		0.2485	7.315	14.65
	4.0202	110.7	18.29		0.3922	11.68	14.66
	4.2498	118.7	18.51		0.5892	17.85	14.70
	4.4968	127.6	18.73		0.7821	24.11	14.73

Table I. *(Continued)*

T (K)	P (MPa)	ρ ($\mathrm{kg \cdot m^{-3}}$)	η ($\mu\mathrm{Pa \cdot s}$)	T (K)	P (MPa)	ρ ($\mathrm{kg \cdot m^{-3}}$)	η ($\mu\mathrm{Pa \cdot s}$)
373.15	0.9797	30.76	14.74	398.15	2.6102	85.93	16.45
	1.1789	37.74	14.80		2.8641	96.59	16.65
	1.3787	45.04	14.85		3.1750	110.5	16.92
	1.5856	52.94	14.94		3.4382	123.0	17.20
	1.7996	61.55	15.04		3.6697	134.8	17.46
	1.9928	69.73	15.12		3.9274	148.7	17.82
	2.2402	80.86	15.29		4.1971	164.5	18.30
	2.4171	89.34	15.44		4.4462	180.2	18.74
	2.6248	99.94	15.59		4.6935	197.2	19.27
	2.8219	110.8	15.84		4.8961	212.3	19.76
	3.0315	123.2	16.06		5.0878	227.7	20.29
	3.2840	139.8	16.46	423.15	0.1025	2.621	16.51
	3.4998	155.9	16.87		0.2957	7.637	16.50
	3.7323	175.7	17.44		0.4904	12.79	16.52
	3.9135	193.6	17.97		0.6849	18.05	16.56
	4.1185	217.7	18.79		0.8796	23.42	16.60
	4.2899	242.8	19.77		1.0802	29.08	16.65
	4.4441	271.9	21.07		1.3217	36.07	16.71
	4.5277	292.1	22.15		1.5655	43.32	16.81
	4.5660	303.0	22.75		1.7613	49.29	16.87
	4.5831	308.3	23.07		1.9576	55.43	16.93
398.15	0.1020	2.776	15.58		2.2205	63.89	17.08
	0.2939	8.069	15.58		2.4178	70.43	17.18
	0.4902	13.68	15.62		2.6316	77.72	17.31
	0.6832	19.31	15.66		2.8522	85.46	17.43
	0.9308	26.77	15.71		3.1893	97.76	17.70
	1.1732	34.33	15.76		3.4662	108.3	17.92
	1.4280	42.59	15.81		3.8083	122.0	18.24
	1.6548	50.22	15.93		4.0588	132.5	18.47
	1.8871	58.35	16.02		4.3248	144.1	18.80
	2.1581	68.25	16.18		4.5926	156.4	19.11
	2.4295	78.68	16.32		4.8256	167.5	19.47

REFPROP [17]. As shown in our previous study [18], no change was observed for the viscosity values due to the density values used for the data analysis based on Newell's theory [19].

The samples were prepared in a sample vessel by charging first the less volatile constituent gas (HFC-134a) and then the more volatile one (HFC-32). When the sample gas mixture was loaded into the viscometer vessel, the temperature of the sample vessel and the connecting tubing between the sample vessel and the viscometer vessel were thermostatted at about 423 K to prevent condensation. Temperature and pressure values have an uncertainty of 0.01 K and 0.5 kPa, respectively. The compositions of the sample mixtures were determined by weighing. The uncertainty of the composition determination was estimated to be less than 10^{-4} mole fraction. Based on the uncertainties of these properties, the uncertainty of the viscosity data is estimated to be within 0.3%.

The HFC-134a and HFC-32 were supplied by Asahi Glass Co. Ltd. The purities of both samples, certified by the suppliers, were approximately 99.9 mol%. The samples were further purified by distillation several times before preparing mixture samples.

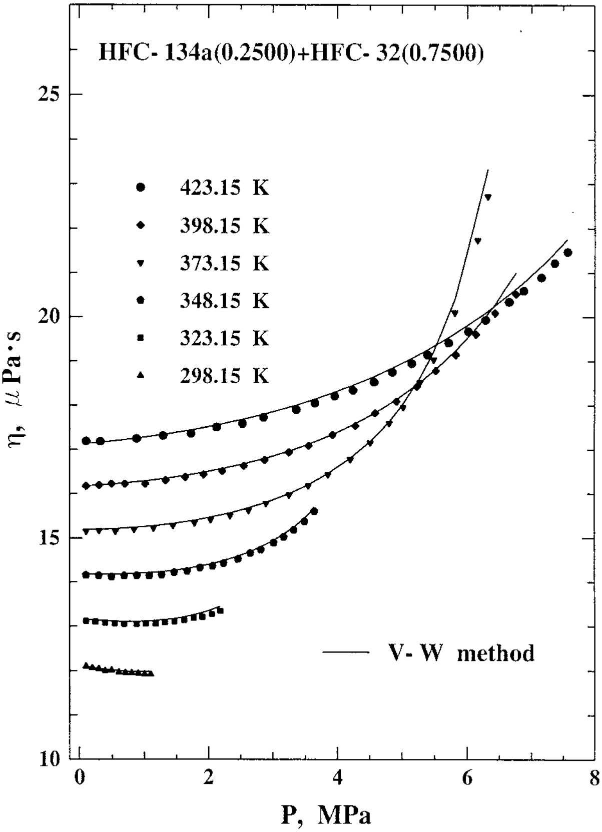

Fig. 1. Viscosity of the binary gaseous mixture of HFC-134a (0.2500) + HFC-32 (0.7500) as a function of pressure.

3. RESULTS AND DISCUSSION

The experimental results for the viscosity of the HFC-134a + HFC-32 system are presented in Table I. The viscosity values of the mixture of HFC-134a (0.2500) + HFC-32 (0.7500) are shown in Figs. 1 and 2. As seen in Fig. 1, the curves as a function of pressure intersect for the isotherms from 348.15 to 423.15 K, but the curves as a function of density do not, as seen in Fig. 2. The initial negative density slope was observed for the viscosity isotherms at 298.15 and 323.15 K. Almost the same behavior was observed in the other two mixtures and also for the pure HFCs and the binary systems (HFC-125/134a and HFC-125/32) studied in our previous studies [1–6].

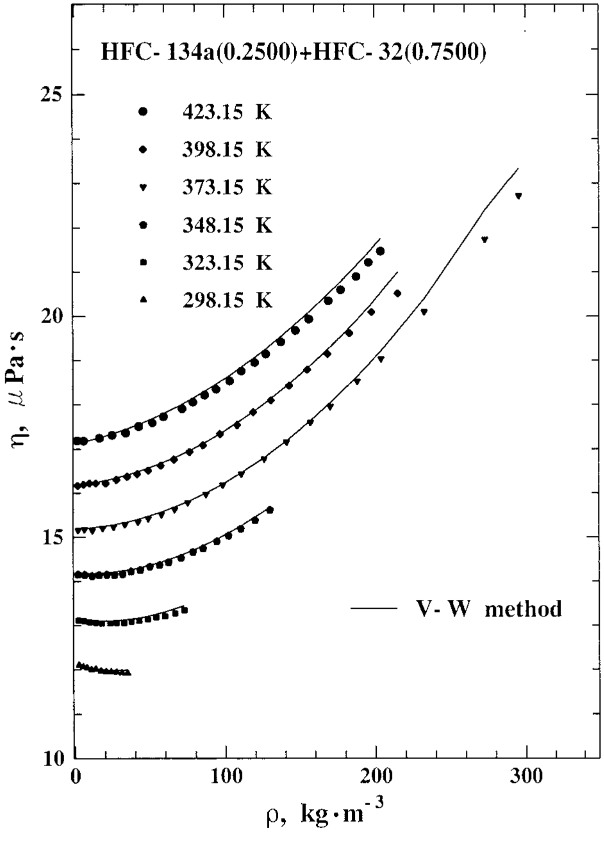

Fig. 2. Viscosity of the binary gaseous mixture of HFC-134a (0.2500) + HFC-32 (0.7500) as a function of density.

The viscosity of gaseous mixtures at 0.1 MPa, η_0, are plotted as a function of mole fraction in Fig. 3, in which the viscosities of HFC-32 [1] are also shown. As can be seen in Fig. 3, the shape of the curves for η_0 is slightly monotonically convex downward in the present experimental temperature range. Moreover, a minimum can be observed at temperatures above 323.15 K. Generally, the viscosity-composition curves are not straight and many mixtures show maxima. Azumi [20] and Hirschfelder et al. [21] developed the theoretical analysis to predict the conditions where the viscosity of a dilute binary gaseous mixture either has a maximum or minimum with respect to variations in the composition. Hirshfelder et al. [21] found that the minimum should occur for a mixture of two nonpolar gases in which both the viscosities and molar masses of the pure components are nearly equal, for which the present binary system

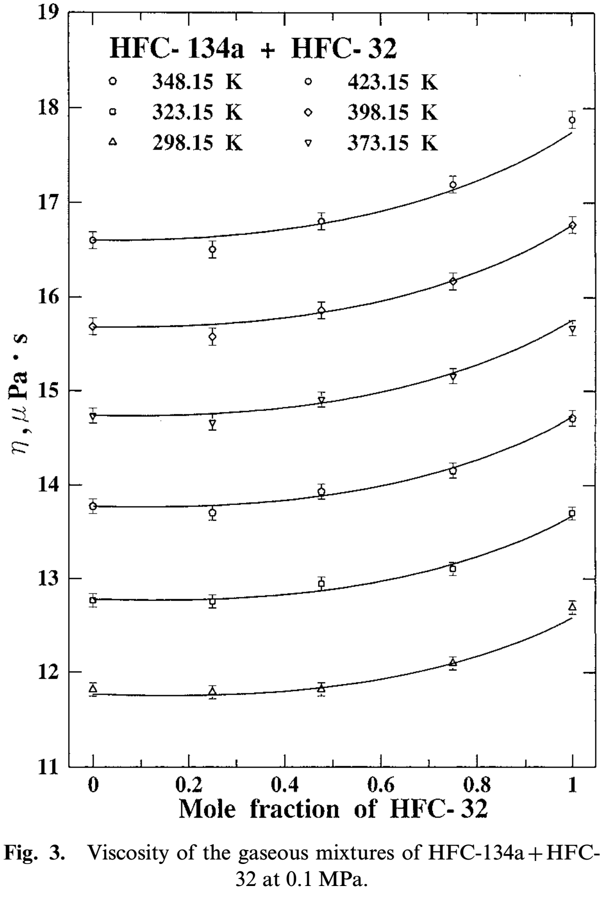

Fig. 3. Viscosity of the gaseous mixtures of HFC-134a+HFC-32 at 0.1 MPa.

does not satisfy this condition. To the best of our knowledge, the HFC-134a+HFC-32 system is the first binary HFC system to show the minimum in the η_0 versus mole fraction plot. In order to make sure of a minimum point, we should make additional viscosity measurements in a composition range from 0.0 to 0.4 of $x_{\mathrm{HFC\text{-}32}}$.

The extended law of corresponding states for the transport properties was applied to determine the scaling parameters for the binary interaction between HFC-134a and HFC-32. The equations used are the same as given by Kestin et al. [7]. The scaling parameters of HFC-134a and HFC-32 are determined from a least-squares fit to the viscosity data for each of the pure HFCs reported previously [1, 4]. The optimum values of the scaling parameters between the HFC-134a and HFC-32 pair interaction are determined with the use of the viscosity data measured in this study. The values of the scaling parameters obtained are shown in Table II. The calculated results with the parameters in Table II are shown as the solid lines in Fig. 3. It can be seen from Fig. 3 that the composition dependence of η_0 is well represented by the extended law of corresponding states with the scaling parameters in Table II. The calculated results also show the minima at 398.15 and 423.15 K, although the calculated mole fractions at the minima are very close to pure HFC-134a. The average absolute deviation between the experimental viscosity values and the calculated results is 0.40%, and the maximum deviation is 1.42%.

The viscosity under pressure is analyzed with the extended Enskog theory developed by Vesovic and Wakeham (V–W method) [8]. In the V–W method, we need the equations for the viscosity of pure constituent gases at 0.1 MPa and under pressures, and for mixture gases at 0.1 MPa. The viscosities at 0.1 MPa are obtained from the extended law of corresponding states described above. The viscosities of pure HFC-134a and HFC-32 are calculated with a residual viscosity equation expressed as follows;

$$\eta-\eta_0=a_1(\rho-\rho_0)+a_2(\rho-\rho_0)^2+a_3(\rho-\rho_0)^3 \qquad (1)$$

Table II. Scaling Parameters for HFC-134a and HFC-32

$i-j$	ε/k (K)	σ (nm)
HFC-134a–HFC-134a	278.31	0.50788
HFC-32–HFC-32	277.46	0.41530
HFC-134a–HFC-32	303.63	0.46199

Table III. Constants in Eqs. (1)–(4)

	HFC-134a	HFC-32
a_{10}	1.956757×10^{-5}	1.581357×10^{-5}
a_{11}	3.250649×10^{-2}	3.667580×10^{-2}
a_{12}	-1.427287×10	-1.511928×10
a_{20}	2.137635×10^{-6}	2.629959×10^{-6}
a_{21}	-1.799517×10^{-3}	-2.049982×10^{-3}
a_{22}	4.047065×10^{-1}	4.362916×10^{-1}
a_{30}	-3.915070×10^{-6}	-2.413426×10^{-6}
a_{31}	3.203120×10^{-3}	1.236867×10^{-8}
a_{32}	-6.530407×10^{-1}	-1.602793×10^{-11}

and

$$a_1 = a_{10}T + a_{11} + a_{12}/T \tag{2}$$

$$a_2 = a_{20}T + a_{21} + a_{22}/T \tag{3}$$

$$a_3 = a_{30} + a_{31}/T + a_{32}/T^2 \tag{4}$$

where η is the viscosity under pressure in μPa · s, η_0 is the gas viscosity at 0.1 MPa in μPa · s, ρ is the gas density under pressure in kg · m^{-3}, ρ_0 is the gas density at 0.1 MPa in kg · m^{-3}, T is the absolute temperature in K, and a_{ij} are adjustable parameters. The values of a_{ij} for HFC-134a and HFC-32 are shown in Table III. While Eqs. (1)–(4) represent the experimental viscosity values with average absolute deviations of less than 0.20% for HFC-134a and 0.19% for HFC-32 in our experimental region, as shown in Table IV, they should not be used at temperatures and/or densities outside of our experimental conditions.

Table IV. Correlation Results of Eq. (1) for HFC-134a and HFC-32

	n.d.[a]	BIAS (%)[b]	AAD (%)[c]	MAX (%)[d]
HFC-134a	127	−0.038	0.181	0.8
HFC-32	115	0.016	0.299	1.0

[a] n.d.: number of data

[b] BIAS (%) $= \sum (\eta_{\text{exp}} - \eta_{\text{cal}})/\eta \times 100/\text{n.d.}$

[c] AAD (%) $= \sum |(\eta_{\text{exp}} - \eta_{\text{cal}})|/\eta_{\text{cal}} \times 100/\text{n.d.}$

[d] MAX (%) = maximum of AAD.

In the V–W method, the mean free path shortening factor, α_{ii}, and the switch-over density are obtained from the following relation,

$$(d\eta_i/d\rho)|_T = \eta_i/\rho \tag{5}$$

In the lower temperature range below 348.15 K, the switch-over densities at which Eq. (5) is valid are much higher than the maximum density of the present experimental conditions. Therefore, Eqs. (1)–(4) should not be applicable to Eq. (5). Thus, the Lee–Thodos (LT) viscosity correlation [22] was applied to Eq. (5). In the LT correlation, we used the extended law of corresponding states to calculate the viscosity at 0.1 MPa and treated the triple-point temperature as the adjustable parameter in order to improve the agreement between the experimental viscosity and correlated results. The optimum value of the triple point temperature was 172.95 K for HFC-134a and 162.06 K for HFC-32.

As for the mixture viscosity calculations, the pseudo-radial distribution function χ_{ij} for species i and j in the mixture should be evaluated. Kestin and Wakeham [23] proposed an equation for χ_{ij} with the use of the density expansion equation for the radial distribution function of hard-sphere fluid mixtures. They used the density expansion equation truncated after second-order density terms. In our previous study [6], we proposed a new method to calculate the χ_{ij} from the exact theoretical equation for the radial distribution functions for the hard-sphere fluid mixture proposed by Carnahan and Starling [9]. As shown by Vesovic and Wakeham [8], the pseudo-radial distribution function for pure gases, χ_i, can be obtained from the pure-component viscosity by application of the hard-sphere expression for the viscosity of a pure gas [Eqs. (6) and (7) in Ref. 8]. We assumed that the χ_i is equal to the Carnahan–Starling radial distribution function of pure hard-sphere fluid i as follows:

$$\chi_i = \frac{1}{(1-\xi_3)} + \frac{3\xi_3^2}{2(1-\xi_3)^2} + \frac{\xi_3^3}{2(1-\xi_3)^3} \tag{6}$$

where ξ_3 is a reduced density defined by $(1/6)\,\pi\rho N_{\mathrm{AV}}\,d_i^3$, ρ is a molar density in $\mathrm{mol\cdot cm^{-3}}$, N_{AV} is Avogadro's number in $\mathrm{mol^{-1}}$, and d_i is a hard-sphere diameter for species i in cm. Once the value of χ_i was obtained from the pure-component viscosity data, the d_i can be determined from Eq. (6). Equation (6) can be expressed as a cubic equation for ξ_3, as shown in Eq. (7):

$$\xi_3^3 - 3\xi_3^2 + \left(3 - \frac{1}{2\chi_i}\right)\xi_3 + \left(\frac{1}{\chi_i} - 1\right) = 0 \tag{7}$$

Since Eq. (7) has only a single real root under the present experimental conditions, the hard-sphere diameter value can be obtained from the following analytical equation:

$$\xi_3 = \frac{\pi}{6} \rho d_i^3 = \left(-\frac{n}{2} + \sqrt{D}\right)^{1/3} + \left(-\frac{n}{2} - \sqrt{D}\right)^{1/3} \tag{8}$$

where

$$D = \frac{n^2}{4} + \frac{m^3}{27} \tag{9}$$

$$n = \frac{27}{2\chi_i} \tag{10}$$

$$m = -\frac{1}{2\chi_i} \tag{11}$$

Once the hard-sphere diameters for every constituent species in the mixture are determined from Eqs. (8)–(11), the pseudo-radial distribution functions for species i and j in the mixture were obtained from the Carnahan–Starling radial distribution function of hard-sphere mixtures [9]. In the case of binary mixture of species i and j, the following equation holds:

$$\chi_{ij} = \frac{1}{(1-\xi_3)} + \frac{3(d_i d_j)\, \xi_2}{(d_i + d_j)(1-\xi_3)^2} + \frac{2(d_i d_j)^2\, \xi_3^2}{(d_i + d_j)^2\,(1-\xi_3)^3} \tag{12}$$

The reduced density ξ_k ($k = 2, 3$) for the binary mixture ($i + j$) is defined as follows:

$$\xi_k = \left(\tfrac{1}{6}\right) \pi \rho N_{\mathrm{AV}} (x_i d_i^k + x_j d_j^k) \tag{13}$$

where x_i is the mole fraction of species i. Since the Carnahan–Starling equation can give accurate results for the thermophysical properties for highly dense hard-sphere fluids, it is reasonable to consider that we can extrapolate the $\chi_{ij}(\rho, T)$ to higher densities.

Comparison between the calculated results from the V–W method with the original mixing rule for χ_{ij} [8] and those with the mixing rule described in this study [Eqs. (6)–(13)] are shown in Table V. The solid lines in Figs. 1 and 2 show the prediction results by the V–W method with the mixing rule shown in Eqs. (6) to (13). Deviation plots based on the calculated values from the mixing rules of Eqs. (6) to (13) are shown in Fig. 4. The deviations of the three mixtures from the two mixing rules for χ_{ij} (ρ, T) are almost the same order of magnitude. This suggests that the mixing rule for $\chi_{ij}(\rho, T)$

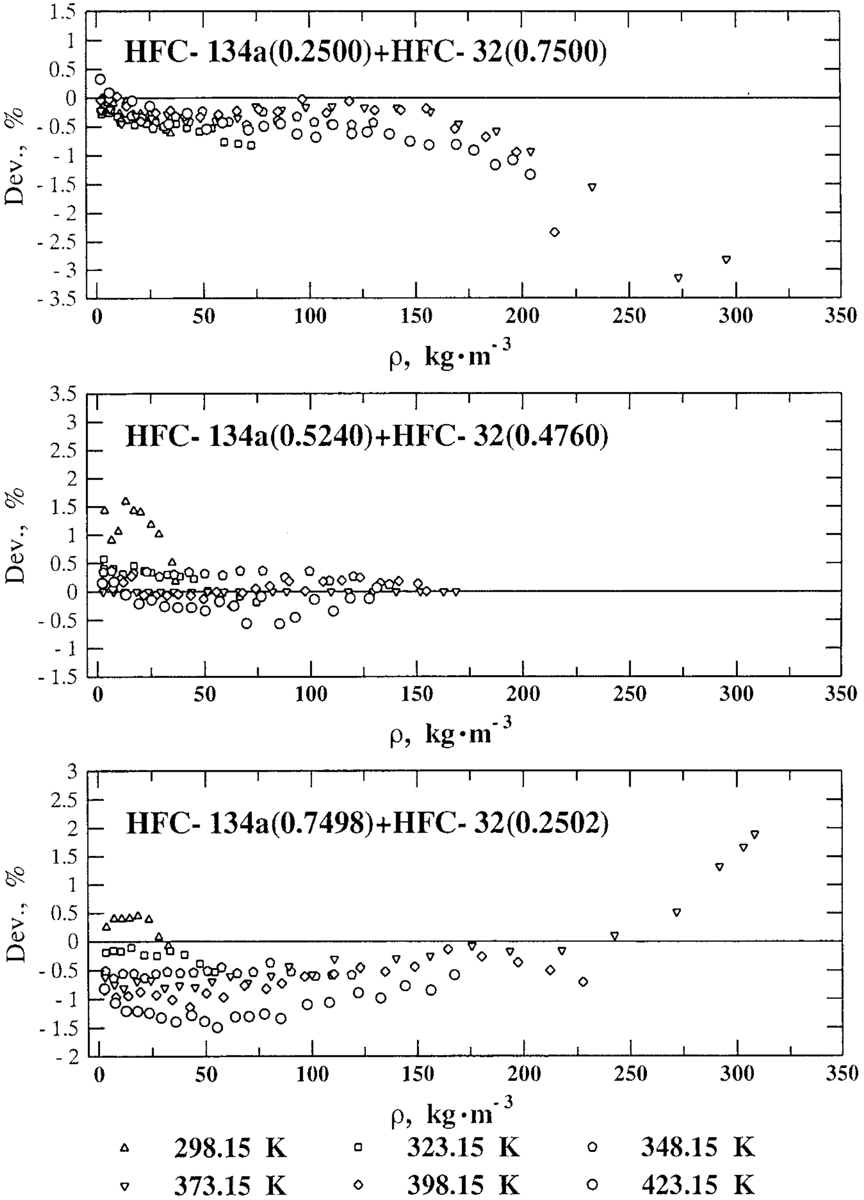

Fig. 4. Deviation plots for the HFC-134a + HFC-32 system. Dev. (%) = $(\eta_{exp} - \eta_{cal})/\eta_{cal} \times 100$.

Table V. Prediction Results of VW Method with Two Mixing Rules for HFC-134a+HFC-32 Mixtures

		original mixing rule for χ_{ij}			mixing rule of Eqs. (6)–(13)		
$X_{\text{HFC-134a}}$	n.d.[a]	BIAS (%)[b]	AAD (%)[c]	MAX (%)[d]	BIAS (%)	AAD (%)	MAX (%)
0.7498	106	−0.523	0.672	1.89	−0.528	0.675	1.86
0.5240	107	0.207	0.317	1.43	0.199	0.310	1.59
0.2500	116	−0.456	0.464	2.66	−0.466	0.474	3.14

[a] n.d.: number of data

[b] BIAS (%) $= \sum (\eta_{\text{exp}} - \eta_{\text{cal}})/\eta \times 100/\text{n.d.}$

[c] AAD (%) $= \sum |(\eta_{\text{exp}} - \eta_{\text{cal}})|/\eta_{\text{cal}} \times 100/\text{n.d.}$

[d] MAX(%) = maximum of AAD.

proposed in this study is almost equivalent to the original mixing rule of Kestin and Wakeham in the present experimental conditions. The ability of the V–W method to represent the density and temperature dependence of the viscosity for the HFC binary mixture may depend mainly on the viscosity correlations used for pure constituent HFCs and also on the density correlations for the HFC mixture.

From the present study for the HFC-134a+HFC-32 system, and our previous studies for the HFC-125/32 and HFC-125/134a systems [5, 6], we have completed an effort to determine all the values of the required parameters for the V–W method for the HFC-125/134a/32 ternary system.

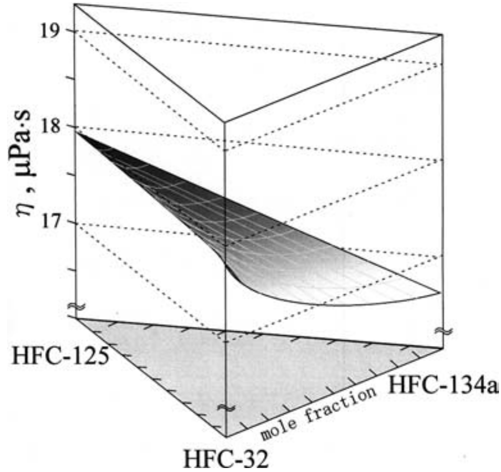

Fig. 5. Prediction of gaseous viscosity for the HFC-125/134a/32 system at 423.15 K and 0.1 MPa.

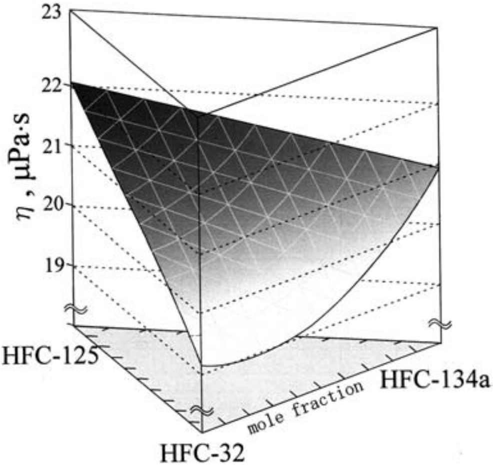

Fig. 6. Prediction of gaseous viscosity for the HFC-125/134a/32 system at 423.15 K and 5 MPa.

Figures 5 and 6 show the calculated results for the gaseous viscosity for the ternary system at two conditions (423.15 K and 0.1 MPa, and 423.15 K and 5 MPa) from the Vesovic–Wakeham method in conjunction with the mixing rule of Eqs. (6)–(13). The gaseous density was obtained from the corresponding state method based on the BWR equation of states for the pure constituent HFCs [24–26]. We have measured the viscosity of the HFC-125/134a/32 ternary systems (R-407C and R-404A) to check the applicability of the V–W method to multicomponent systems which will be reported soon. We are now planning to compare the experimental density values of the binary and ternary gaseous mixtures of HFCs and the calculated density values with the corresponding state theory.

4. CONCLUSION

In this paper, we report experimental results for the gaseous viscosity for the HFC-134a + HFC-32 system. It was found that the viscosity at 0.1 MPa for the binary mixture shows minima in the higher temperature region, i.e., above 348.15 K. The scaling parameters for the molecular interaction between HFC-134a and HFC-32 were determined with the extended corresponding state theory and the viscosity data at 0.1 MPa. The viscosity values of the gaseous mixture under pressure were predicted with the modified Enskog theory developed by Vesovic and Wakeham. The pseudo-radial distribution functions needed for the viscosity predictions were determined from the method based on the exact equation for radial distribution functions for hard-sphere fluids developed by Carnahan and Starling and also the numerical method developed by Kestin and Wakeham. From the comparisons between the calculated results and the experimental viscosity values, both methods give almost the same results for the present experimental conditions. We can conclude that the Vesovic–Wakeham method should be a reliable method for viscosity predictions for mixtures of HFCs under pressure, for the case for viscosities of pure HFCs under pressure and of gaseous HFC mixtures under normal pressure and also when the density of gas mixtures under pressure can be predicted and/or correlated with high accuracy. The prediction results for the ternary system of HFC-125/134a/32 are presented.

ACKNOWLEDGMENTS

The authors acknowledge suggestions of an anonymous reviewer which improved the manuscript significantly. This study was supported from the research project entitled "Infrastructure development of thermophysical properties data for future industries" organized by Japan Space Utilization Promotion Center (JSUP) and New Energy Industrial Technology Development Organization (NEDO), which is gratefully acknowledged.

REFERENCES

1. M. Takahashi, N. Shibasaki-Kitakawa, C. Yokoyama, and S. Takahashi, *J. Chem. Eng. Data* **40**:900 (1995).
2. N. Shibasaki-Kitakawa, M. Takahashi, and C. Yokoyama, *Int. J. Thermophys.* **19**:1285 (1998).
3. M. Takahashi, N. Shibasaki-Kitakawa, and C. Yokoyama, *Int. J. Thermophys.* **20**:435 (1999).
4. M. Takahashi, N. Shibasaki-Kitakawa, and C. Yokoyama, *Int. J. Thermophys.* **20**:445 (1999).
5. C. Yokoyama, T. Nishino, and M. Takahashi, *Fluid Phase Equilib.* **174**:231 (2000).
6. C. Yokoyama, T. Nishino, and M. Takahashi, *Int. J. Thermophys.* **22**:1329 (2001).
7. J. Kestin, K. Knierim, E. A. Mason, B. Najafi, S. T. Ro, and M. Waldman, *J. Phys. Chem. Ref. Data* **13**:229 (1984).
8. V. Vesovic and W. A. Wakeham, *Int. J. Thermophys.* **10**:125 (1989).
9. N. F. Carnahan and K. E. Starling, *J. Chem. Phys.* **51**:635 (1969).
10. M. Takahashi, C. Yokoyama, and S. Takahashi, *J. Chem. Eng. Data* **33**:267 (1988).
11. M. Takahashi, C. Yokoyama, and S. Takahashi, *Trans. JAR* **6**:57 (1989).
12. C. Yokoyama, M. Takahashi, and S. Takahashi, *Int. J. Thermophys.* **15**:603 (1994).
13. K. Stephan, R. Krauss, and A. Laesecke, *J. Phys. Chem. Ref. Data* **16**:993 (1987).
14. R. T Jacobsen and R. T. Stewart, *J. Phys. Chem. Ref. Data* **2**:757 (1973).
15. L. A. Weber, *Int. J. Thermophys.* **15**:461 (1994).
16. L. A. Weber and D. R. Defibaugh, *Int. J. Thermophys.* **15**:863 (1994).

17. REFPROP, NIST REFPROP DATABASE Version 6.01, Nat. Inst. Stds. Tech., Boulder, Colorado (1998).
18. C. Yokoyama and M. Takahashi, *Int. J. Thermophys.* **21**:695 (1999).
19. G. F. Newell, *ZAMP* **10**:160 (1959).
20. H. Azumi, *Bull. Chem. Soc. Japan* **12**:199 (1937).
21. J. O. Hirschfelder, M. H. Taylor, T. Kihara, and R. Rutherford, *Phys. Fluids* **4**:663 (1961).
22. H. Lee and G. Thodos, *Ind. Eng. Chem. Res.* **29**:1404 (1990).
23. J. Kestin and W. A. Wakeham, *Ber. Bunsenges. Phys. Chem.* **84**:762 (1980).
24. H. Sunaga, R. Tillner-Roth, H. Sato, and K. Watanabe, *Int. J. Thermophys.* **19**:1623 (1998).
25. R. Tillner-Roth and H. D. Baehr, *J. Phys. Chem. Ref. Data* **23**:657 (1994).
26. R. Tillner-Roth and A. Yokozeki, *J. Phys. Chem. Ref. Data* **26**:1273 (1997).